9

Large surface nanostructuring by lithographic techniques for bioplasmonic applications

Gregory Barbillon, Frederic Hamouda, Bernard Bartenlian

Institute of Fundamental Electronics CNRS UMR 8622, University of Paris-Sud, Orsay, France;

Outline:

Introduction

The realization of high density nanostructures over large surfaces is very important point for the biochemical sensing based on localized surface plasmon resonance of metallic nanostructures. In order to study multiple biomolecular interactions on the same surface, very large substrate areas need to be fabricated. Various techniques such as electron beam lithography are available to design these large surfaces. However, these techniques are expensive and slow to obtain these surfaces. Moreover, charge effect on insulating surface can alter the regularity of the pattern shape. Thus, these techniques are not suitable for a large scale production. Other lithographic techniques such as deep UV lithography are also used, but these techniques (fabrication of masks) are expensive and allow with difficulty to realize samples in small quantity. In addition, alternative methods emerged, and among these methods we find nanosphere lithography and nanoimprint lithography. These two techniques are fast to carry out high density nanostructures, not very expensive and compatible with biological and biochemical applications. The aim of this chapter is to present the principle of these various fabrication techniques for the plasmonic nanostructure realization on large surfaces (from few mm^2 to some cm^2), and the advantages and disadvantages of these four usual techniques : electron beam lithography, deep UV lithography, soft UV nanoimprint lithography and nanosphere lithography.

Conventional lithographies

Electron Beam Lithography

The electron beam lithography is a technique of micro/nanofabrication, which use an electron beam to insolate an electrosensitive resist deposited on a sample of which the surface will be micro/nanostructured. The trajectory of electron beam follows a pattern realized by a suitable software. Each pattern is realized point by point. After development, the resist can be used as mask and integrate a “classical” process of micro/nanofabrication: dry or wet etching, lift-off or others. The spatial resolution depends on the characteristics of the electron beam (current, energy), of the nature of the sample and the used resist. Typically, a resolution of 20 nm is obtained (with a system RAITH 150) with PolyMethylMethAcrylate (PMMA), which is a positive-tone resist, i.e. the insolated part is removed with the development. This resist is well-suitable to the fabrication of plasmonic nanostructures. On figure 9.1 is represented the principle of electron beam lithography used for the realization of plasmonic nanostructures. The initial step consists into a deposit by spin-coating the PMMA on a substrate of glass thoroughly cleaned. The used PMMA has typically a molecular mass of 950K. The deposited thickness of PMMA depends on acceleration, the speed of the spin-coating but also of the concentration of the PMMA (example: PMMA A2 (Anisole solvent)). The selected parameters allow to obtain a suitable height of PMMA. This deposited thickness choice depends on the height of the structures to realize. The “rule” is to obtain a ratio of 1:3 between the height of the structures to be realized and the thickness of the PMMA. The second step aims to withdraw the solvent (Anisole) film of PMMA. An annealing of the sample at 180°C during 20 minutes is thus carried out. Then, the sample must be made conductive to avoid the charge effects (accumulation of the electrons on a given zone). To avoid these charge effects, a layer of aluminum of 10 nm is deposited on the layer of PMMA [1-3]. Other solutions can be used such as conductive polymers.

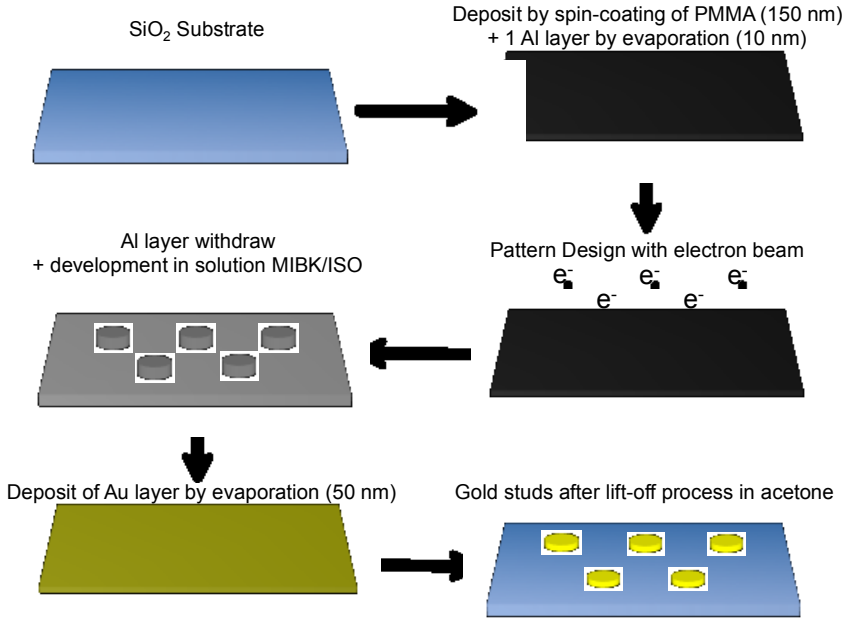

FIGURE 9.1
Fabrication principle of plasmonic nanostructures by electron beam lithography on glass substrate

The step of writing is realized by the electron beam. The acceleration voltage of electrons typically used is of 20 kV for a system RAITH 150. This voltage permits to obtain a good resolution. Then, the layer of aluminum is dissolved by using a potash solution (KOH). Next, the sample is developed and that consists of a dissolution of the insolated zones of the PMMA having a lower molecular mass due to the breaks of the polymer chains after the writing step. A solution of 1:3 of MethylIsoButylKetone (MIBK) and isopropanol is used for the development in order to obtain a very good resolution [4-7]. Then, the metal thickness, typically 50 nm, is evaporated. Finally, the last step aims to remove the remaining PMMA via a lift-off process, which consists to dip the sample in acetone. After all these steps, the plasmonic nanostructures are thus obtained. An example of plasmonic nanostructures is displayed on the figure 9.2. Advantages of the electron beam lithography on the other conventional lithography techniques such as the optical lithographies "classic" and "Deep UV", are the realization of exotic patterns of triangle type, antenna "bowtie" with very small periodicity and size (Ex: 20 nm diameter for studs with 50 nm of periodicity). However, the major disadvantage of the electron beam lithography is its writing time when large zones of some mm^2 or cm^2 are to be insolated. To give an example of writing time, a zone of 1 mm^2 take approximately 12h of insolation with a system RAITH150 which is a very powerful system of lithography with a relatively high purchase price (magnitude order of price : 600000 euros). There exist obviously systems more powerful as NanoBeam nB5 (NANOBEAM LTD) which would insolate this zone of 1 mm^2 with a writing time of one hour but it is very expensive (approximately 1 million euros).

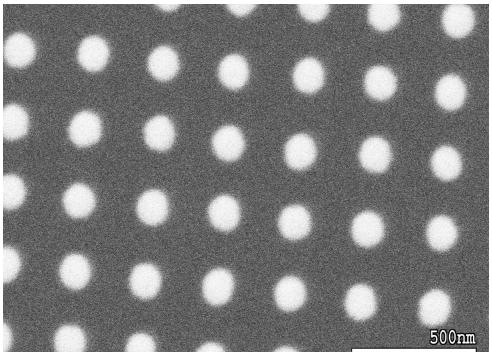

FIGURE 9.2
SEM image of example of plasmonic nanostructures realized by electron beam lithography on glass substrate, with following dimensions (gold studs): 100 nm of diameter, 50 nm of height and 300 nm of periodicity

To avoid this constraint of writing time for large surfaces (≥ mm^2) to insolate, other techniques exist such as the nanoimprint lithography, which is a unconventional lithographic technique. This technique will be presented in the paragraph 3.1.2. Now, we present the technique of the deep UV lithography (other conventional lithography), which has a short writing time compared to EBL.

Deep UV Lithography

As electron beam lithography and focused-ion-beam (FIB) milling have large writing times, they are not very suitable for large-scale development of plasmonic micro/nanostructures for biosensing. Other techniques such as nanosphere lithography (presented in the paragraph 3.2) do not allow reproductible development of micro/nanostructures. In this case, Deep UV lithography (DUV) can be used and it is a reduced projection lithography technology based on 193 nm wavelength deep ultraviolet (see figure 9.3(a)). Development of DUV lithography is currently underway for the mass production of devices for ArF dry and immersion exposures for 65 nm to 22 nm design rule applications. Table 9.1 displayed the relationship among technology node (R), exposure numerical aperture (NA) and process coefficient factor (k_1). The feature resolution R is defined by the Rayleigh's criterion : $R = (k_1\lambda/NA)$. However, the development of DUV exposure equipment presents some disadvantages as the development of ArF immersion exposure system. We report the use of this technique of Deep UV lithography for the development of plasmonic substrates.

TABLE 9.1
Relationship at a wavelength of 193 nm, among technology node (R), numerical aperture (NA), and process coefficient factor (k_1)

R	65 nm	45 nm	32 nm	22 nm
NA	k_1	k_1	k_1	k_1
0.93	0.31			
1	0.4			
1.2		0.28		
1.35		0.31	0.22	0.15

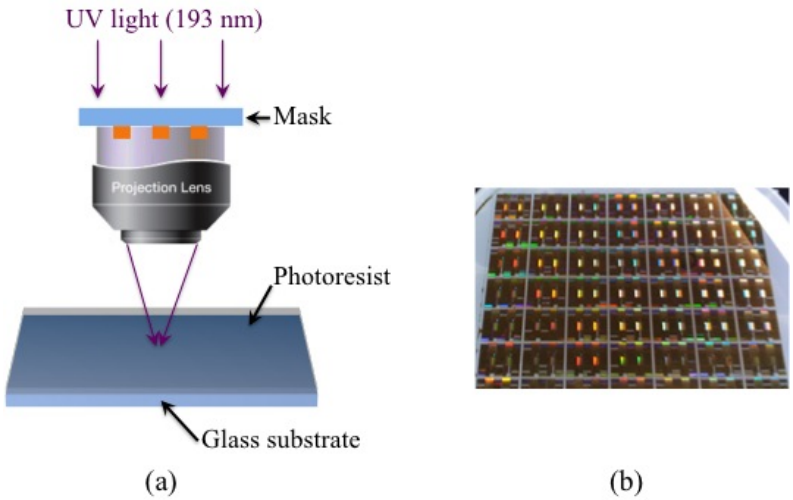

FIGURE 9.3
(a) Principle of deep UV lithography, (b) Image of a 6-inch wafer containing several gold micro/nanoline chips on glass substrate

In the example presented here, the plasmonic structures consist of gold micro/nanolines fabricated on glass wafers. The first fabrication step of the gold micro/nanolines involved exposure of a positive photoresist (spin-coated on a 6 inch wafer, see figure 9.3(b)) by using deep UV lithography [8]. Before deposit of the photoresist, an antireflective coating was deposited on top of the wafer. An photoresist of 200 nm is used in order to allow for an easier lift-off process. An ASML 5500/950B scanner (ArF 193 nm radiation) was used for the deep UV lithography. The deep UV lithography mask was designed such that various structure periods and gap sizes between the nanolines were present on the same substrate varying between 100 nm and 10 µm. An exposure dose of 25 $mJ.cm^{-2}$ was chosen in order to obtain the desired sizes, gaps of the micro/nanolines for the plasmonic structures [8]. After the photoresist exposure and development, the antireflective coating film was removed by reactive ion etching (RIE). Then, an adhesion layer of titanium (~5 nm) and a thin gold film (~50 nm thick) were evaporated in the gaps. A lift-off process is realized to withdraw the unexposed photoresist in NMP (*N*-methyl pyrrolidone) solution at 80°C. Next, they were rinsed with acetone and methanol and then dried with a nitrogen gun. Finally, RIE of polymer was done for 3 min to ensure that the entire photoresist polymer has lifted off. Thus, the plasmonic structures were obtained on large area with this technique of DUV. Figure 9.4 displays SEM images of gold micro/nanolines obtained by DUV with the following dimensions : (a) gap = 103 nm / period = 300 nm, (b) gap = 56 nm / period = 1655 nm [8].

In conclusion, the deep UV lithography enables the production of plasmonic structures on large surface with a good spatial resolution. However, the mask cost is very expensive. In order to obtain a better spatial resolution, a development of ArF immersion exposure system is necessary, which is also a disadvantage. To avoid these disadvantages, the technique of nanoimprint lithography emerged such as UV nanoimprint lithography, which is not very expensive and compatible with biological applications [9,10].

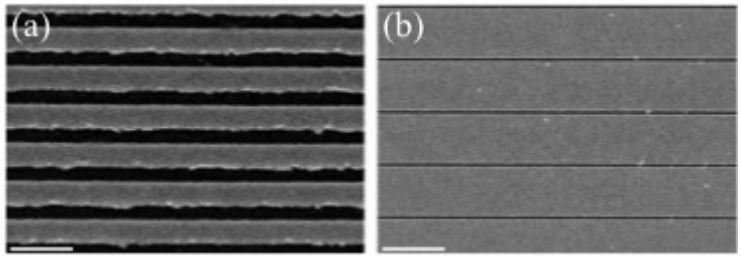

FIGURE 9.4
SEM images of an gold micro/nanolines example fabricated by Deep UV lithography with different gap sizes/structure periods: (a) 103 ± 10 nm / 300 ± 9 nm (scale bar = 500 nm), (b) 56 ± 5 nm / 1655 nm ± 10 nm (scale bar = 2 μm)

Unconventional lithographies

Nanoimprint Lithography

The lithography is a basic step in the processes of micro-and nano-fabrication. The main fonction is to structure patterns in a polymer that was previously deposited on a substrate and allows other process like etching or deposit materials. At present, the developed technologies use conventional lithography techniques such as optical lithography or e-beam lithography. Beyond these technologies, other modes of unconventional low cost, such as NanoImprint Lithography (NIL), has been developed to be also be used. The NIL technique is based on the printing patterns in a polymer using a mold which may be rigid or flexible. This method was developed in the 90s because it allowed obtaining quickly and at low cost networks nanoscale patterns over large areas. The main steps are imprint in the polymer with a mold, and after separation, transfer the pattern in the substrate. As presented in figure 9.5, there are two main technics in the NIL. The first method developed was a thermal process more commonly known as hot embossing. *S.Y.Chou* published the first results of this technique in 1995 [11].
A second method, the UV-NIL appears few years later, it was developed in research laboratories Philips. The photon energy is used to crosslink the resist. This process requires transparent molds and it offers other advantages compared to thermal NIL. We will detail the UV-NIL and more specifically the soft UV-NIL in the next paragraph.

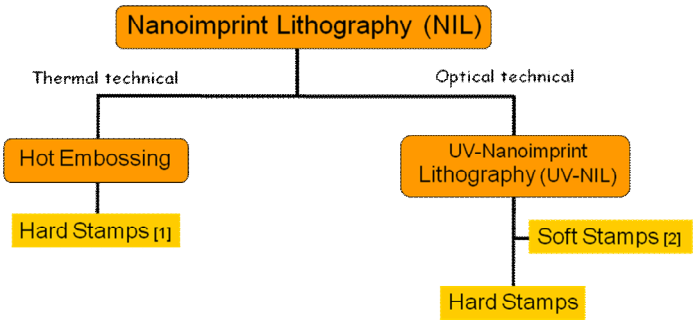

FIGURE 9.5
Main ways of the NanoImprint Lithography

Thermal NIL

The thermal NIL process is to imprint patterns in a thermoplastic polymer using a structured rigid master mold [11]. Figure 9.6(a) summarizes the basic steps. They require the fabrication of a mold pattern by controlling the depth, the selection of a polymer to be heated to a temperature above its glass transition temperature (Tg), and the use of a press which allows to perform pressures up to 200 bar [12]. This technique achieves resolutions in the nanometer range. However, it has the disadvantage of using high temperatures to achieve a temperature above transition temperature and high pressures until 200 bar.

UV-NIL

With these constraints, pressure and thermal treatment, a new technique has been developed, the UV-NIL, where the cross linking of the resist is achieved through the photon energy. This optical path proposes one method based on a transparent flexible mold (Soft UV-NIL). Figure 9.6(b) summarizes this way of soft UV Nanoimprint Lithography. Unlike thermal NIL, UV-NIL requires low pressure, and is realized at room temperature.

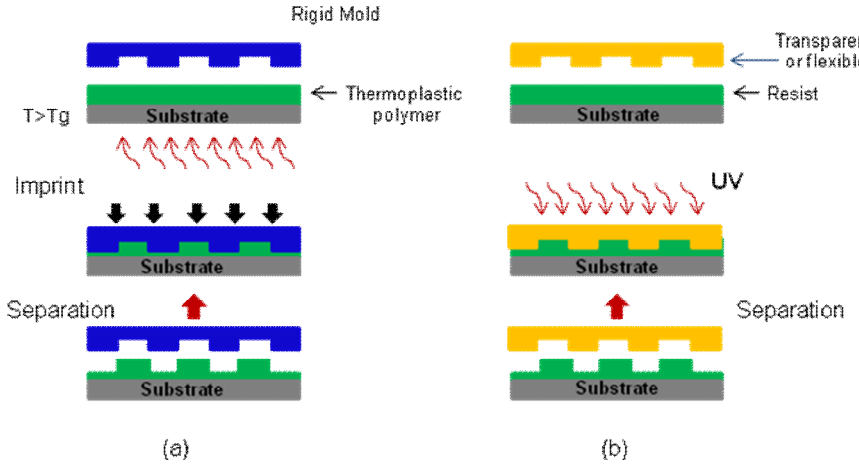

FIGURE 9.6
Principle of thermal NIL (a), and UV-NIL (b)

Soft UV-NIL

The UV-NIL has two fundamental steps and is illustrated in figure 9.6(b). Firstly, a UV-transparent mold with the desired patterns on its surface is imprint in the UV-sensitive resist. This resist, which is liquid at room temperature, is typically deposited by spin-coating on the substrate. Then, the transparent mold is deposited on the substrate with a low pressure ranging between 0 and 1 bar [13], at room temperature. Then, the transparent mold is removed. The first step duplicates the patterns of the transparent mold in UV-sensitive resist. The second step is to withdraw the residual layer of UV resist. This step is carried out by an anisotropic etching such as RIE (Reactive Ion Etching) in order to obtain the desired patterns in UV resist. During the nanoimprint step, the resist is cured by a UV source (for example, a simple UV lamp or other systems available). The main advantages of the UV-NIL are the use of a flexible transparent mold and a low viscosity UV-curable resist. The replication of the transparent molds is typically obtained by molding and curing of a polymer from a 3D template. The realization of the UV-transparent flexible mold is generally carried out with the polymer poly(dimethylsiloxane) PDMS [14]. The PDMS offers a good chemical stability and a high optical transparency [15]. Moreover, the deformation risk of the transparent mold is minimized with the use of UV-resist which has a low viscosity, and allows a 3D-structuring at low pressure without any cycle of heating.

Different steps of soft UV-NIL

The complete fabrication of plasmonic nanostructures is divided as follows: (1) the realization of the master mold, (2) the fabrication of the UV-transparent flexible mold, (3) the step of nanoimprint in UV resist with the transparent flexible mold.

Fabrication of the Si master mold

The master mold used to realize the transparent flexible mold is carried out with EBL. EBL allows an excellent accuracy, very a high-resolution and a capacity to make a large variety of geometries. In the example presented here for the master mold in Si, a layer of PMMA (Ex: PMMA A6) is deposited by spin-coating on the Si substrate and annealed at 180°C during 30 min. A system of electron beam lithography RAITH 150 is used to expose the PMMA A6, by employing a acceleration voltage of 20 kV, an aperture of 7.5 µm and a working distance of 7 mm. Then, the sample is developed in a solution of MIBK/ISO with room temperature for 35 s followed by a rinsing of 10 s in isopropanol and thoroughly dried with nitrogen. Then, the patterns designed in the PMMA are transferred in the Si substrate via a suitable RIE. The conditions of RIE for the pattern transfer are available in the following references [13,16]. The mask of PMMA is then removed with a lift-off process in trichloroethylene at 80°C. The surface of the Si master mold is treated with hydrofluoric acid (HF) and hydrogen peroxide H_2O_2 in order to obtain a thin surface of SiO_2, then modified with an anti-adhesive layer (TMCS: TriMethylChloroSilane) to decrease the surface energy (Si+TMCS = 28.9 mN/m) in order to easily withdraw the PDMS transparent molds [16-18]. In figure 9.7, SEM images of nanostructures obtained on the Si substrate are presented. For the master mold of the example presented here, the hole dimensions obtained are ~160 nm of diameter and a periodicity of ~500 nm on a zone of 1 mm^2.

In addition, we developed an alternative method with the electron beam lithography in order to carry out the master mold. This technique uses the anodic aluminum oxide (AAO) membranes. These AAO substrates display an arrangement of nanometric pores organized in hexagonal structure on very large surfaces (Ex: a few cm^2). The dimensions of vertical pores can be easily tuned like the diameter and the

aspect ratio. The order of magnitude of the diameter is from 10 to 200 nm and the aspect ratio can be higher than 500. The synthesis of the alumina membranes is electrochemically carried out from aluminum wafers. After polishing, the anodic potential is applied to the aluminum wafer at controlled temperature, and immersed in an acid bath. The important parameter is the anodization voltage for the growth of these highly ordered nanoporous membranes. In the presented example, experimental conditions were chosen to obtain membranes with thicknesses of approximately 10 μm and hole diameters of 180 nm (see figure 9.8) [19,20]. Thus, we can obtain gold nanodisks by using the alumina membranes for the fabrication of the transparent flexible molds [21].

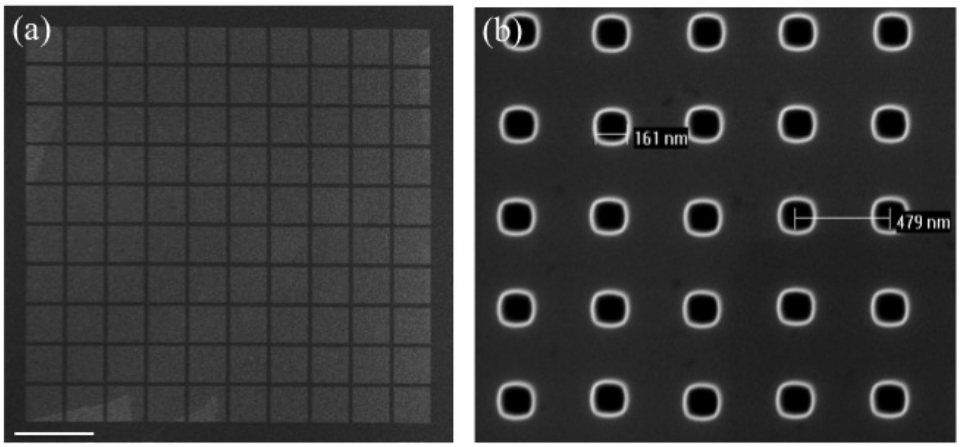

FIGURE 9.7
SEM images of a Si master mold by electron beam lithography: (a) zone of 1 mm^2 (scale bar = 200 μm), (b) nanohole zoom, diameter 160 nm and periodicity ~ 500 nm)

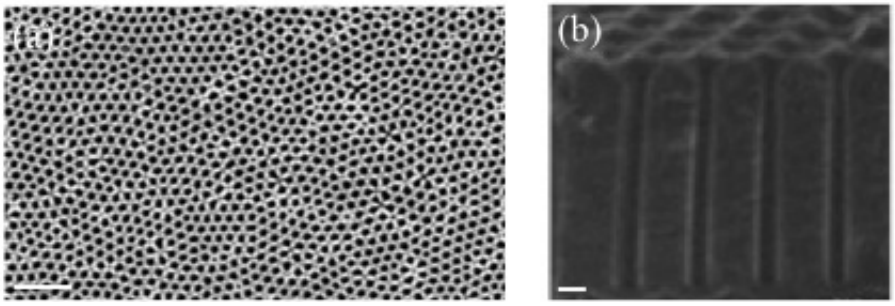

FIGURE 9.8
SEM images of AAO templates: (a) Large view of nanopores (scale bar = 10 μm), (b) Height profile of these vertical nanopores (scale bar = 200 nm).

Fabrication of the UV-transparent flexible mold

To obtain a good resolution and fidelity of the structures, the mechanical properties of the transparent mold were improved. Indeed, Odom *et al.* [22] developed a bilayer mold of Hard-PDMS and standard PDMS which present like advantages, a rigid layer to obtain a pattern transfer with a high-resolution

and an elastic support for obtaining a contact which follows the pattern design even at low pressure. The Hard-PDMS has an attractive property: a lower viscosity of its prepolymer in comparison with the standard PDMS. The viscosity of the prepolymer is obtained by decreasing its chain length during its preparation. Thus, the replication accuracy is particularly improved for small structures with high density. Other groups [23,24] also studied the viscosity reduction of the prepolymer for a good replication of the master mold. In this case, the viscosity of the prepolymer of the PDMS was decreased with the introduction of a solvent into the mixture. This solvent used with an excess of modulator allows to delay the PDMS curing.

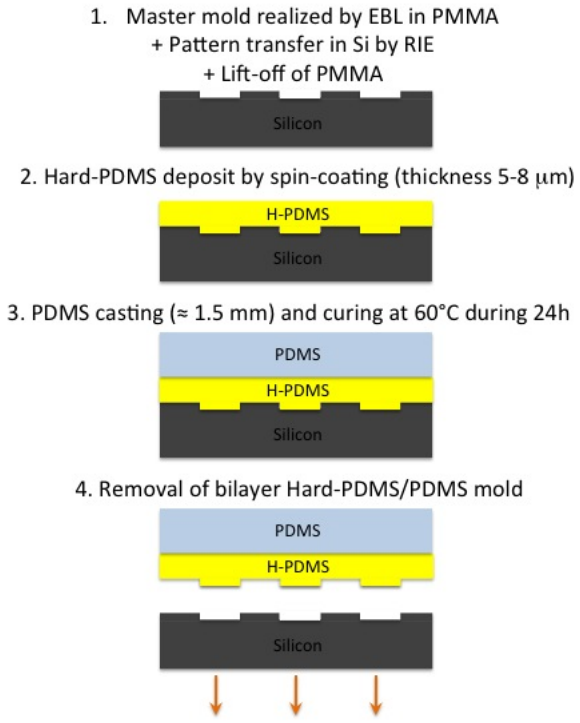

FIGURE 9.9
Principle scheme of the fabrication process of the hard-PDMS/PDMS stamp

Figure 9.9 represents the fabrication process of the bilayer mold Hard-PDMS/PDMS. The Hard-PDMS is a specific thermocured siloxane polymer based on copolymers: Vinylmethylsiloxane-Dimethylsiloxane (VDT301) and Methylhydrosilane-Dimethylsiloxane (HMS-301) from ABCR [25]. Then, the Hard-PDMS is deposited by spin-coating on the Si master mold and the thickness used is generally of 5-8 μm and this layer of Hard-PDMS is supported by a standard layer of PDMS (~1.5 mm). The layer of standard PDMS keeps a good flexibility and adaptation on the spin-coated substrate during the imprint transfer [26]. Then, the bilayer mold is on a glass carrier. The standard PDMS (RTV 615) with its curing agent is mixed before the deposit on the thin Hard-PDMS layer. To finish, the sample is cured at 60°C during 24 hours and treated with an anti-adhesive layer of TMCS. For the chosen example of nanostructures, this type of flexible mold is very suitable. Indeed, dimensions of the studs are 160 nm of diameter and a

periodicity of 500 nm. Figure 9.10(a) represents an AFM image of the obtained transparent bilayer mold.

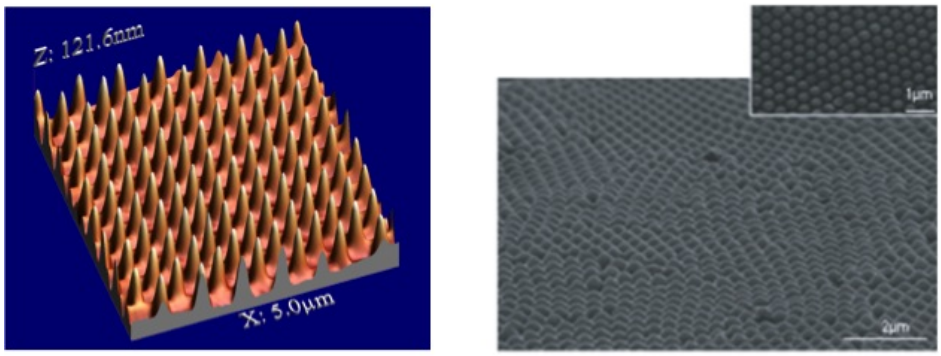

FIGURE 9.10
(a) AFM image of the dots in H-PDMS stamp (periodicity: ~ 500 nm, diameter (FWHM): ~ 160 nm and height: 150 nm), (b) SEM image of stamp of PDMS hexane diluted at 5%, tilted at 55°, and the insert shows a top view

In addition, SEM images of figure 9.10(b) show the nanostructured surface of the diluted PDMS with hexane (at 5%) of a surface of approximately 100 μm^2 by using the nanoporous alumina membranes (AAO) for the fabrication of the transparent mold. The topography of the AAO master molds was indeed transferred in the transparent mold in PDMS on several cm^2. The mold is composed of micro-domains of regularly organized nanobumps. Each bump has a height of 180 nm and a diameter of 250 nm. For this fabrication, the PDMS was simply spread on the AAO membranes without additional pressure, but with its own weight. Before this step, the standard PDMS with its curing agent and solvent (hexane) were mixed and cured at 60°C during 12 hours. The thickness of the layer of PDMS obtained is approximately 3 mm. After curing, the layer is peeled off manually. An advantage of using the alumina membranes is their low reactivity of surface compared with the surface of SiO_2. Thus, the anti-adhesive layer is not necessary and the possible interactions with the used solvent can be avoided, when molding and demolding PDMS from AAO membranes.

Nanoimprint in AMONIL with the flexible UV-transparent mold

Several UV-sensitive resists exist like the NXR 2010 and the AMONIL. These two resists exhibit a good performance for the resolution and resistance to etching. The AMONIL was chosen for its low cost compared to the NXR 2010, its excellent time of conservation and the AMONIL is a mixture of organic compounds and inorganic having a surface energy of 39.5 mN/m. AMONIL MMS4 from AMO GMBH is used and deposited by spin-coating on the top of an underlayer of PMMA A2 (100 nm of thickness, surface energy = 40.2 mN/m) which is the etching mask for the final step of RIE and allows the lift-off of AMONIL after curing. For our example, a thickness of AMONIL of 120 nm is chosen. Then, the imprint process is realized in AMONIL with an UV exposure at a wavelength of 365 nm and with a power of 10 mW/cm^2 during a exposure time of 20 min. The pressure used to imprint is of 200 mbar. All these parameters were optimized for the fabrication of nanostructures, which uses the flexible mold

obtained with the Si master mold. Figure 9.11(a) represents the imprint in AMONIL. The dimensions obtained for the nanoholes imprinted in AMONIL are ~160 nm of diameter and ~500 nm of period and these values are in good agreement with dimensions of the nanoholes of the Si master mold.

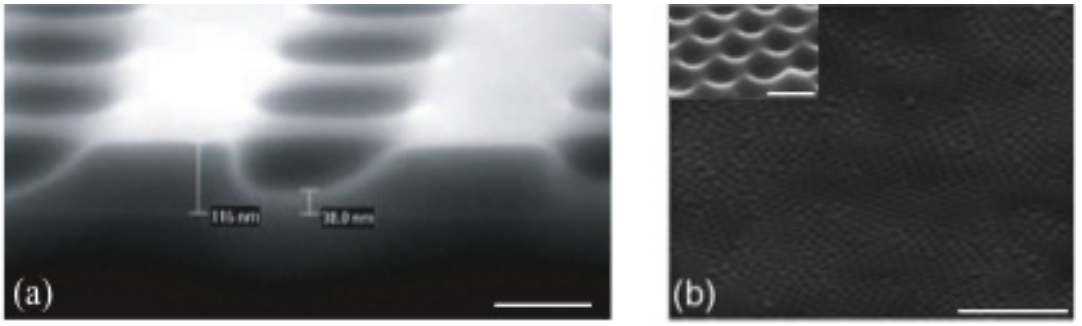

FIGURE 9.11
SEM images of an imprint in AMONIL resist: (a) with flexible stamp obtained from the Si master mold (scale bar = 200 nm), and (b) from AAO master mold, imprint on large area (scale bar = 5 μm), and the insert is an image zoom of imprint (scale bar = 500 nm)

Concerning the transparent mold obtained with the AAO membranes, the thicknesses of PMMA and AMONIL are 130 nm and 150 nm, respectively. The imprint pressure is realized by simple deposit of the transparent mold in standard PDMS on the top of the AMONIL layer without any additional pressure (or external). Only its own weight (~1g) ensures the imprint. For a transparent mold in PDMS of 1 cm^2, that corresponds to a pressure of approximately 70 Pa [14]. Figure 9.11(b) represents the topography of the AMONIL layer after molding. This topography of surface is very similar to the AAO master mold. During the imprint, the transparent mold penetrates completely in the AMONIL layer. The thickness of this layer is lower than the height of the prepared bumps. Thus, these results prove the feasibility of imprint in AMONIL using the transparent molds realized with the alumina membranes on large surfaces (cm^2). However, the diameters of the nanoholes obtained for the imprint in AMONIL are larger (diameter ~ 250 nm) that those obtained with the AAO master mold. This difference is due to the bad penetration of the PDMS in the nanoholes. We demonstrated that the penetration was better when the PDMS is well-diluted with hexane [21]. Fabrication process improvements of these transparent molds must be done.

Fabrication of plasmonic nanostructures

Firstly, the residual thickness of AMONIL in the ground of the nanoholes must be withdrawn by an suitable RIE before the etching of the underlayer of PMMA. Indeed, this residual thickness is of approximately 40 nm (see figure 9.11(a)). For the removal of the residual layer, the used etching gases are O_2 and CHF_3. For the withdrawal of the PMMA A2, the used gas is O_2. A good selectivity between the PMMA and the AMONIL is obtained [13,16]. The next step is the evaporation of a thin layer of gold (30 nm for the structures carried out from the Si master mold and 50 nm from the AAO master mold) in order to carry out plasmonic nanostructures. As a preliminary, an adhesion layer (Cr) for gold is evaporated (3-5 nm). Then, a lift-off in acetone is used to withdraw the underlayer of PMMA (+AMONIL) in order to obtain gold nanostructures. All these conditions of etching, deposit and top lift-off are valid for the 2 types of sample. Moreover, an annealing at 250°C during 30 min to smooth and

compact nanostructures is carried out. Only the sample of gold nanostructures obtained with the Si master mold was annealed. Figure 9.12 presents the results obtained with the 2 fabrication methods. Dimensions of gold nanostructures are in good agreement with those obtained for the imprint in AMONIL for the 2 methods. Indeed, the nanostructure diameters are 165 nm and 250 nm, respectively. On the SEM image of the figure 9.12(a), we observe that annealing have smoothed and compacted the gold studs compared with SEM image of the figure 9.12 (b), where the gold studs are not annealed.

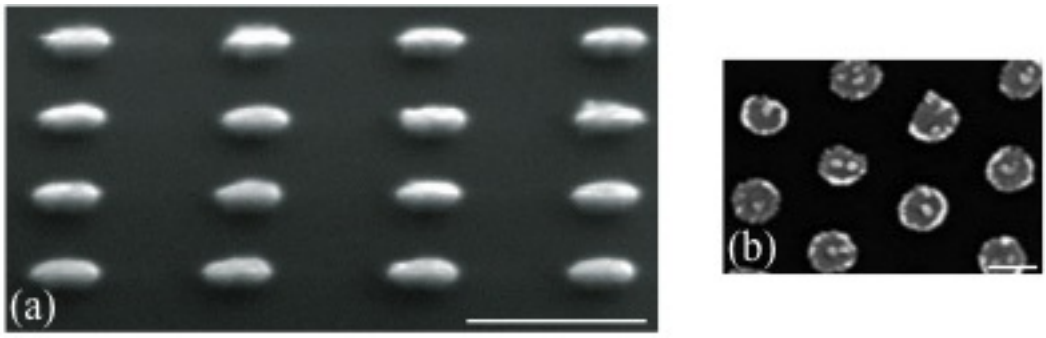

FIGURE 9.12
SEM images of gold nanodisks with the following dimensions: (a) diameter = 165 nm, height = 30 nm and the periodicity = 500 nm (scale bar = 500 nm), and the image is tilted by 60°, and (b) diameter = 250 nm, height = 50 nm and the image is tilted by 45° (scale bar = 250 nm)

To summarize, the technique of the soft UV nanoimprint lithography is divided in 3 steps: the fabrication of the master mold, the replication of the Hard-PDMS/PDMS flexible transparent mold from the master mold, and the imprint process by using the bilayer Hard-PDMS/PDMS mold. All these stages are very important in order to obtain very a good quality of the final result, in terms of resolution and roughness of line edge of nanostructures. The capacity of the UV-NIL to replicate nanostructures with a great homogeneity on all surface was demonstrated. The resolutions in terms of size and periodicity which could be obtained with this technique of UV-NIL (but not exhaustive) are a diameter of approximately 20 nm and a pitch of approximately 60 nm on a large zone [27]. The technique of the soft UV nanoimprint lithography is very promising and relatively simple to employ in order to carry out plasmonic nanostructures on large surfaces (Ex: mm^2 or cm^2). Next, the nanosphere lithography is presented. This technique is also low cost and simplest to implement.

Nanosphere Lithography

Nanosphere lithography (NSL), also called Colloidal Lithography, is not very expensive, simple to implement, capable to produce well-ordered 2D nanoparticle arrays on large surface. NSL was demonstrated to be well-suited to the fabrication of size-tunable metallic nanoparticles in the 20-1000 nm range [28]. Each structure obtained by NSL starts with the self-assembly of size-monodisperse nanospheres with a diameter D in order to realize a two-dimensional colloidal mask (Figure 9.13). To deposit a nanosphere solution onto the substrate, several methods exist such as spin coating [29], drop coating [30], and thermoelectrically cooled angle coating [31]. The nanospheres must be freely spread across the substrate with a configuration of the lowest energy. This phenomena is often obtained by chemical modification of the nanosphere surface. This chemical modification can be realized with a negatively charged functional group such as carboxylate or sulfate, which is electrostatically repulsed

by the negative surface charges of substrate such as glass. The nanospheres assemble into a 2D hexagonal lattice on the substrate due to the capillary forces during the solvent (water) evaporation. Nanosphere masks can include some defects that are due to nanosphere polydispersity, site randomness, and others. Sizes of the defect domain are in the 10-100 μm^2 range. After the step of the nanosphere mask self-assembly, a metallic layer of the fixed and controlled thickness (Ex : gold for bioplasmonic applications) is typically evaporated by electron beam deposition normally to the substrate through the nanosphere mask (Figure 9.13). Then, the nanosphere mask is removed by sonicating the sample in a solvent. Thus, plasmonic nanostructures are obtained (Figure 9.14).

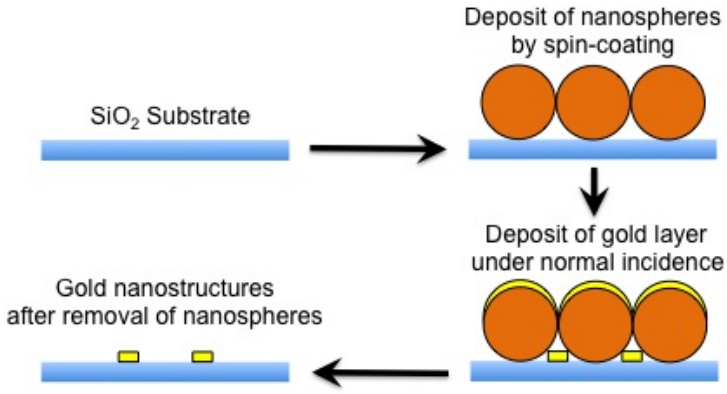

FIGURE 9.13
Principle of Nanosphere Lithography

Two ways of fabrication for NSL can be used in order to obtain nanostructure arrays, which are a single or double layer of nanospheres. This part describes how nanoparticle size, shape, and arrangement can be significantly altered to realize new patterns with small modifications of NSL. In first NSL configuration, only a nanosphere monolayer is deposited and self-assembled onto the substrate (Figure 9.14 (a)). When the gold layer is deposited through the monolayer mask, the three-fold interstices enable gold to reach the substrate, giving an array of triangular nanoparticles with a *P6mm* symmetry. In this case, nanostructures cover around 7% of the substrate area. The single layer of nanospheres is the most used for the nanostructure fabrication. Figure 9.14(a) displays an example of nanostructures obtained by NSL (single layer of nanospheres).

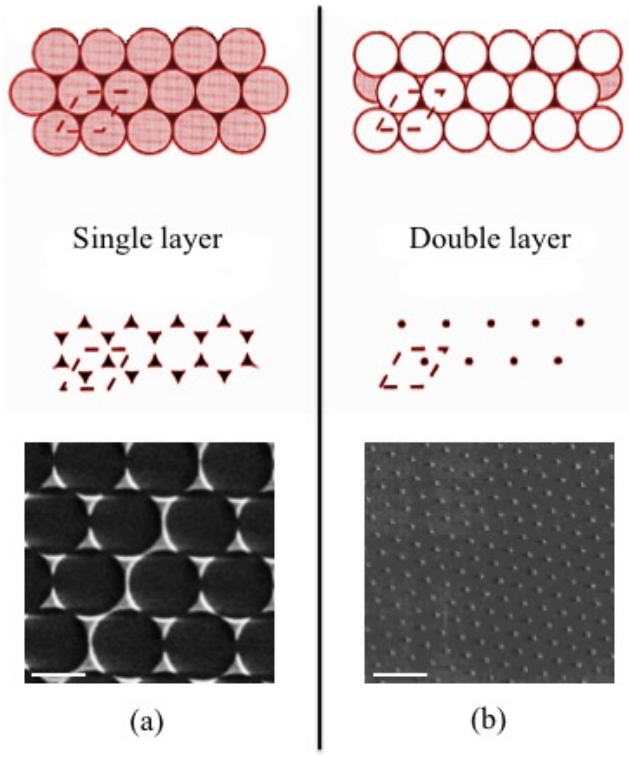

FIGURE 9.14
Schematic representation of single (a) and double layer (b) with associated SEM images of gold nanostructures obtained with the two ways of NSL (for (a) scale bar = 400 nm, and for (b) scale bar = 1 μm)

For the second NSL configuration, double layer of nanospheres is deposited and assembled onto the substrate. This is realized by an increasing of the nanosphere concentration in the solution to be self-assembled onto the substrate in order to obtain a significant part of a double layer of hexagonally assembled nanospheres. When other nanosphere layer is assembled onto the first, each other 3-fold interstice is blocked and only the 6-fold interstices are « open » with a weaker density (Figure 9.14(b)). After the step of gold evaporation through the double layer of nanospheres (mask), the mask is withdrawn, and a homogeneous pattern of hexagonal nanoparticles is obtained on the substrate. As in the case of a single layer of nanospheres, the size of the double layer nanoparticles can be tuned by the deposited nanosphere size (diameter D) and the evaporated thickness of metal. In this case, nanostructures cover around 2% of the substrate area. Figure 9.14(b) displays an example of nanostructures obtained by NSL (double layer of nanospheres).

Others NSL structures can be fabricated by varying the deposition angle between the nanosphere mask and the beam of material being deposited. This technique is called angle-resolved NSL (AR NSL). Angle tuning was used previously to nanostructure other surfaces, such as field effect transistors [32,33] and optical coatings [34]. This technique enables to obtain nanooverlap structures or nanogap structures (see reference [28] for more details).

To summarize, the technique of the nanosphere lithography is simple to implement, low cost. Large surface patterning can be obtained, and NSL offers the possibility to produce in mass samples. However, the spatial resolution is lower to the EBL. The EBL resolution remains the best one. Other point for NSL, the assembly of nanospheres can present some defects, which reduce the patterning accuracy.

Conclusions

In this chapter, we presented the principle of four usual techniques of lithography : the electron beam lithography (EBL), the deep UV lithography (DUV), the soft UV nanoimprint lithography (UV-NIL), and to finish the nanosphere lithography (NSL). The main advantages and disadvantages of 4 lithographic techniques are presented in Table 9.2. We remark that the best spatial resolution is obtained by EBL, but other lithographic techniques have also a good spatial resolution (SR), which is relatively close to that of the EBL. With EBL, various shapes, sizes can be obtained on large surface. However, the writing time is long in order to realize large surface patterning, and EBL is a very expensive technique. For DUV, the main advantage to compare with EBL is the writing time. In order to obtain a better spatial resolution in DUV, an immersion exposure system must be to implement, which is not simple to install. Concerning to soft UV-NIL, this technique have several advantages to compare to others: a quick writing time, possibility of imprint on corrugated surface, a mass production of samples, and this technique is also low cost. Nevertheless, the SR of soft UV-NIL is excellent but remains lower than EBL ($SR_{UV\text{-}NIL} < SR_{EBL}$). The last technique presented in this chapter is nanosphere lithography. NSL has various advantages compared to others even for UV-NIL. Indeed, NSL is the simplest of 4 presented techniques. Firstly, NSL is easy to implement and low cost. Large area can be nanostructured and there is not writing time for the nanostructure fabrication as for the optical or electronic lithographies. Moreover, NSL can produce in mass samples with a good SR. Nevertheless, the assembly of nanospheres in NSL technique can present some defects which decrease the nanostructuring precision. Its spatial resolution is weaker than EBL ($SR_{NSL} < SR_{EBL}$). To finish, several lithographic techniques are at your disposal to realize nanostructures on large area. All depends on your financial supports and the requirements in terms of size for nanostructures to obtain.

TABLE 9.2
Advantages and disadvantages for each presented techniques

Techniques	Advantages	Disadvantages
EBL	- High spatial resolution - Various Shapes - Large surface patterning	- High cost - Writing time for large surface - Charge effects on insulating substrates - Mass production
Deep UV	- Short exposure time - Good spatial resolution - Large surface patterning	- High cost of mask - Resolution < EBL resolution - Mass production - Immersion exposure system for better resolution
Soft UV-NIL	- Writing time (imprint) - Large surface patterning - Imprint on corrugated substrate - Good spatial resolution - Mass production - Low cost	- Resolution < EBL resolution
NSL	- Low cost - Large surface patterning - Good spatial resolution - Mass production	- Defect presence in assembly of nanospheres - Resolution < EBL resolution

References

1. Barbillon G, Bijeon J-L, Plain J, Lamy de la Chapelle M, Adam P-M, Royer P. Electron beam lithography designed chemical nanosensors based on localized surface plasmon resonance. Surface Science 2007; 601 5057-5061.
2. Barbillon G, Bijeon J-L, Plain J, Lamy de la Chapelle M, Adam P-M, Royer P. Biological and chemical gold nanosensors based on localized surface plasmon resonance. Gold Bulletin 2007; 40(3) 240-244.
3. Barbillon G, Bijeon J-L, Bouillard J-S, Plain J, Lamy de la Chapelle M, Adam P-M, Royer P. Detection in near-field domain of biomolecules adsorbed on a single metallic nanoparticle. Journal of Microscopy 2008; 229(2) 270-274.
4. Barbillon G, Faure A-C, El Kork N, Moretti P, Roux S, Tillement O, Ou M G, Descamps A, Perriat P, Vial A, Bijeon J-L, Marquette C A, Jacquier B. How nanoparticles encapsulating fluorophores allow a double detection of biomolecules by localized surface plasmon resonance and luminescence. Nanotechnology 2008; 19 035705.

5. Barbillon G, Ou M G, Faure A-C, Marquette C A, Bijeon J-L, Tillement O, Roux S, Perriat P. Two examples of nanostructured gold surfaces as biosensors. Surface-enhanced chemiluminescence and double detection by localized surface plasmon resonance and luminescence. Gold Bulletin 2008; 41(2) 174-186.
6. Barbillon G, Bijeon J-L, Plain J, Royer P. Sensitive detection of biological species through localized surface plasmon resonance on gold nanodisks. Thin Solid Films 2009; 517 2997-3000.
7. Faure A-C, Barbillon G, Ou M G, Ledoux G, Tillement O, Roux S, Fabregue D, Descamps A, Bijeon J-L, Marquette C-A, Billotey C, Jamois C, Benyatou T, Perriat P. Core/shell nanoparticles for multiple biological detection with enhanced sensitivity and kinetics. Nanotechnology 2008; 19 485103.
8. Dhawan A, Duval A, Nakkach M, Barbillon G, Moreau J, Canva M, Vo-Dinh T. Deep UV nano-microstructuring of substrates for surface plasmon resonance imaging. Nanotechnology 2011; 22 165301.
9. Gates B D, Xu Q, Stewart M, Ryan D, Wilson C G, Whitesides G M. New approaches to nanofabrication: Molding, Printing, and other techniques. Chemical Reviews 2005; 105 1171-1196.
10. Krauss P R, Chou S Y. Nano-compact disks with 400 Gbit/in^2 storage density fabricated using nanoimprint lithography and real with proximal probe. Applied Physics Letters 1997; 71 3174-3176.
11. Chou S Y, Krauss P R, Renstrom P J. Imprint of sub-25 nm vias and trenches in polymers. Applied Physics Letters 1995; 67 3114-3116.
12. Gourgon C, Perret C, Tallal J, Lazzarino F, Landis S, Joubert O, Pelzer R. Uniformity across 200 mm silicon wafers printed by nanoimprint lithography. Journal of Physics D: Applied Physics 2005; 38 70-73.
13. Hamouda F, Barbillon G, Held S, Agnus G, Gogol P, Maroutian T, Scheuring S, Bartenlian B. Nanoholes by soft UV nanoimprint lithography applied to study of membrane proteins. Microelectronic Engineering 2009; 86 583-585.
14. Hamouda F, Barbillon G, Gaucher F, Bartenlian B. Sub-200 nm gap electrodes by soft UV nanoimprint lithography using polydimethylsiloxane mold without external pressure. Journal of Vacuum Science and Technology B 2010; 28(1) 82-85.
15. Schmid H, Biebuyck H, Michel B, Martin O J M. Light-coupling masks for lensless, sub-wavelength optical lithography. Applied Physics Letters 1998; 72 2379-2381.
16. Barbillon G, Hamouda F, Held S, Gogol P, Bartenlian B. Gold nanoparticles by soft UV nanoimprint lithography coupled to a lift-off process for plasmonic sensing of antibodies. Microelectronic Engineering 2010; 87 1001-1004.
17. Shi J, Chen J, Decanini D, Chen Y, Haghiri-Gosnet A-M. Fabrication of metallic nanocavities by soft UV nanoimprint lithography. Microelectronic Engineering 2010; 86 596-599.
18. Chen J, Shi J, Decanini D, Cambril E, Chen Y, Haghiri-Gosnet A-M. Gold nanohole arrays for biochemical sensing fabricated by soft UV nanoimprint lithography. Microelectronic Engineering 2009; 86 632-635.
19. Sengupta K, Moyen E, Macé M, Benoliel A-M, Pierres A, Thibaudau F, Masson L, Limozin L, Bongrand P, Hanbücken M. Large-scale ordered plastic nanopillars for quantitative live-cell imaging. Small 2009; 5 449-453.
20. Masuda H, Fukuda K. Ordered metal nanohole arrays by a two-step replication of Honeycomb structures of anodic alumina. Science 1995; 268 1466-1468.
21. Hamouda F, Sahaf H, Held S, Barbillon G, Gogol P, Moyen E, Aassime A, Moreau J, Canva M, Lourtioz J-M, Hanbücken M, Bartenlian B. Large area nanopatterning by combined anodic

aluminum oxide and soft UV-NIL technologies for applications in biology. Microelectronic Engineering 2011; 88 2444-2446.
22. Odom T W, Love J C, Wolfe D B, Paul K E, Whitesides G M. Improved pattern transfer in soft lithography using composite stamps. Langmuir 2002; 18 5314-5320.
23. Kang H, Lee J, Park J, Lee H H. An improved method of preparing composite poly (dimethylsiloxane) moulds. Nanotechnology 2006; 17 197-200.
24. Koo N, Bender M, Plachetka U, Fuchs A, Wahlbrink T, Bolten J, Kurz H. Improved mold fabrication for the definition of high quality nanopatterns by soft UV nanoimprint lithography using diluted PDMS material. Microelectronic Engineering 2007; 84 904-908.
25. Choi D-G, Yu H-K, Yang S-M. 2D nano/micro hybrid patterning using soft/block copolymer lithography. Materials Science and Engineering C 2004; 24 213-216.
26. Plachetka U, Bender M, Fuchs A, Vratzov B, Glinsner T, Lindner F, Kurz H. Wafer scale patterning by soft UV nanoimprint lithography. Microelectronic Engineering 2005; 73/74 167-171.
27. Cattoni A, Cambril E, Decanini D, Faini G, Haghiri-Gosnet A-M. Soft-UV-NIL at 20 nm scale using flexible bilayer stamp casted on HSQ master mold. Microelectronic Engineering 2010; 87 1015-1018.
28. Haynes C L, Van Duyne R P. Nanosphere Lithography: A versatile nanofabrication tool for studies of size-dependent nanoparticle optics. Journal of Physical Chemistry B 2001; 105 5599-5611.
29. Hulteen J C, Van Duyne R P. Nanosphere Lithography: A Materials General Fabrication Process for Periodic Particle Array Surfaces. Journal of Vacuum Science and Technology A 1995; 13 1553-1558.
30. Hulteen J C, Treichel D A, Smith M T, Duval M L, Jensen T R, Van Duyne R P. Nanosphere Lithography: Size-Tunable Silver Nanoparticle and Surface Cluster Arrays. Journal of Physical Chemistry B 1999; 103 3854-3863.
31. Micheletto R, Fukuda H, Ohtsu M. A simple method for the production of a two-dimensional, ordered array of small latex particles. Langmuir 1995; 11 3333-3336.
32. Dickman J, Geyer A, Daemkles H, Nickel H, Lösch R, Schlapp W. Fabrication of Low Resistance Submicron Gates in Pseudomorphic MODFETS using Optical Contact Lithography. Journal of the Electrochemical Society 1991; 138 491-493.
33. Strifter W A, Cantos B D. An edge-defined technique for fabricating submicron metal-semiconductor field effect transistor gates. Journal of Vacuum Science and Technology B 1990;8 1297-1299.
34. Mbise G W, Le Bellac D, Niklasson G A, Granqvist C J. Angular selective window coatings: theory and experiments. Journal of Physics D: Applied Physics 1997; 30 2103-2122.